

Dispersive analysis for $\eta \rightarrow \gamma\gamma^*$

C. Hanhart^{a,1,2,3}, A. Kupść^{b,4,5}, U.-G. Meißner^{c,1,2,3,6,7}, F. Stollenwerk^{d,1,8}, A. Wirzba^{e,1,2,3}

¹Institut für Kernphysik (Theorie), Forschungszentrum Jülich, D-52425 Jülich, Germany

²Institute for Advanced Simulation, Forschungszentrum Jülich, D-52425 Jülich, Germany

³Jülich Center for Hadron Physics, Forschungszentrum Jülich, D-52425 Jülich, Germany

⁴Division of Nuclear Physics, Department of Physics and Astronomy Uppsala University, Box 516, 75120 Uppsala, Sweden

⁵High Energy Physics Department, National Centre for Nuclear Research, ul. Hoza 69, 00-681 Warsaw, Poland

⁶Helmholtz-Institut für Strahlen- und Kernphysik, Universität Bonn, D-53115 Bonn, Germany

⁷Bethe Center for Theoretical Physics, Universität Bonn, D-53115 Bonn, Germany

⁸Present Address: Institut für Physik, Humboldt-Universität zu Berlin, Newtonstr. 15, D-12489 Berlin, Germany

Received: date / Accepted: date

Abstract A dispersion integral is derived that connects data on $\eta \rightarrow \pi^+\pi^-\gamma$ to the $\eta \rightarrow \gamma\gamma^*$ transition form factor. A detailed analysis of the uncertainties is provided. We find for the slope of the η transition form factor at the origin $b_\eta = (2.05^{+0.22}_{-0.10}) \text{ GeV}^{-2}$. Using an additional, plausible assumption, one finds for the corresponding slope of the η' transition form factor, $b_{\eta'} = (1.58^{+0.18}_{-0.13}) \text{ GeV}^{-2}$. Both values are consistent with all recent data, but differ from some previous theoretical analyses.

Keywords Form factors · Dispersion integral · Vector meson dominance

1 Introduction

Transition form factors contain important information about the properties of the decaying particles. Additional interest into meson decays with one or two virtual photons in the final state comes from the fact that the theoretical uncertainty for the Standard Model calculations for $(g-2)$ of the muon will soon be completely dominated by the hadronic light-by-light amplitudes, where they appear as sub-amplitudes (for a recent discussion of this issue see Refs. [1, 2]).

In this work, using dispersion theory, the connection between the radiative decays $\eta \rightarrow \pi^+\pi^-\gamma$ and $\eta' \rightarrow \pi^+\pi^-\gamma$ and the isovector contributions of the form factors $\eta \rightarrow \gamma\gamma^*$ and $\eta' \rightarrow \gamma\gamma^*$ is exploited in a model-independent way. This is possible, because the amplitude of the former decays can be parametrized in terms of the pion vector form factor, $F_V(Q^2)$, and a low-order polynomial [3], since $F_V(Q^2)$ as

well as the radiative decay amplitudes $\eta \rightarrow \pi\pi\gamma$ and $\eta' \rightarrow \pi\pi\gamma$ share, at least in the low-energy regime, the same right-hand cut. Therefore the vector form factor and the decay amplitudes must agree up to a function that is free of a right-hand cut and therefore varies only smoothly with Q^2 —the invariant mass squared of the pion pair. It was therefore proposed to parametrize the differential decay widths for $\eta \rightarrow \pi\pi\gamma$ (and analogously for $\eta' \rightarrow \pi\pi\gamma$) as

$$\frac{d\Gamma_{\pi\pi\gamma}^\eta}{dQ^2} = |A_{\pi\pi\gamma}^\eta P(Q^2) F_V(Q^2)|^2 \Gamma_0(Q^2), \quad (1)$$

where the normalization parameter $A_{\pi\pi\gamma}^\eta$, which is determined by the empirical value of the partial decay width [4], has the dimension of mass^{-3} . The function

$$\Gamma_0(Q^2) = \frac{1}{3 \cdot 2^{11} \cdot \pi^3 m^3} (m^2 - Q^2)^3 Q^2 \sigma_\pi(Q^2)^3$$

collects phase-space terms and the kinematics of the absolute square of the simplest gauge invariant matrix element (for point-particles). The $\pi\pi$ -two-body phase space reads $\sigma_\pi(Q^2) = \sqrt{1 - 4m_\pi^2/Q^2}$, where m (m_π) denotes the mass of the decaying particle (charged pion).

In order to fit the spectral shape of the radiative η [5] and η' decays [6], a linear polynomial was sufficient for specifying the function $P(Q^2)$ [3]. In addition, the slope extracted from the two fits were consistent within uncertainties—a finding that can be understood using arguments from large N_c chiral perturbation theory. We may therefore write

$$P(Q^2) = 1 + \alpha Q^2, \quad (2)$$

identifying α as a fundamental parameter to characterize the decays $\eta \rightarrow \pi\pi\gamma$ and $\eta' \rightarrow \pi\pi\gamma$.

In this paper we will use the findings of Ref. [3] to make model-independent predictions for the isovector contribution to the $\eta/\eta' \rightarrow \gamma\gamma^*$ transition form factor and its slope

^ae-mail: c.hanhart@fz-juelich.de

^be-mail: Andrzej.Kupsc@physics.uu.se

^ce-mail: meissner@hiskp.uni-bonn.de

^de-mail: felix.stollenwerk@physik.hu-berlin.de

^ee-mail: a.wirzba@fz-juelich.de

at the origin based on a dispersion integral that only needs $P(Q^2)$ as well as $F_V(Q^2)$ as input. This analysis in principle requires knowledge about these quantities up to infinite values of Q^2 ; however, as we will demonstrate in the next sections, the relevant dispersion integral is largely saturated in a regime where we do control the input. In addition, the uncertainties from the kinematic regions where, *e.g.*, the function $P(Q^2)$ is not well known, can be reliably estimated.

The paper is structured as follows: in the next section we will update the analysis of Ref. [3] and also discuss the behavior of $P(Q^2)$ in the complete region $4m_\pi^2 \leq Q^2 \leq 1 \text{ GeV}^2$. In the subsequent section the dispersion integral for the isovector part of the $\eta/\eta' \rightarrow \gamma\gamma^*$ transition form factor and its slope is derived, followed by a discussion of a model for the isoscalar counter part. We close with a presentation of the results and a summary. A comparison with the vector-meson dominance approximation is relegated to the appendix.

2 Remarks on the radiative decays of η and η'

In this section we update the results of Ref. [3] since new data were published in the meantime [7]. In addition, we provide arguments why $P(Q^2)$ can be assumed linear in the whole range of $4m_\pi^2 \leq Q^2 \leq 1 \text{ GeV}^2$.

The discontinuity relation for the pion vector form factor gives

$$\text{Im}(F_V(Q^2)) = \sigma_\pi(Q^2) T_p^*(Q^2) F_V(Q^2) \Theta(Q^2 - 4m_\pi^2), \quad (3)$$

where $\Theta(\dots)$ is the Heaviside step function and $T_p(Q^2)$ denotes the $\pi\pi$ elastic scattering amplitude in the p -wave that may be expressed via the corresponding phase shift $\delta_p(Q^2)$ as

$$T_p(Q^2) = \frac{1}{\sigma_\pi(Q^2)} \sin(\delta_p(Q^2)) \exp(i\delta_p(Q^2)). \quad (4)$$

Below we use the phase shifts from the analysis of Ref. [8].

If one assumes that the two-pion interactions are elastic up to infinite energies, the dispersion integral that emerges from Eq. (3) can be solved analytically yielding the celebrated Omnès function

$$\Omega(Q^2) = \exp\left(\frac{Q^2}{\pi} \int_{4m_\pi^2}^{\infty} \frac{ds}{s} \frac{\delta_p(s)}{s - Q^2 - i\epsilon}\right). \quad (5)$$

Since any function that is multiplied to $F_V(Q^2)$ and that is real on the right-hand cut does not spoil Eq. (3), one may write in general

$$F_V(Q^2) = R(Q^2) \Omega(Q^2). \quad (6)$$

An identical derivation leads us to the analogous expression for the amplitudes for the radiative decays of η and η' , *e.g.*,

$$\mathcal{A}_{\pi\pi\gamma}^\eta(Q^2) = A_{\pi\pi\gamma}^\eta P_\Omega(Q^2) \Omega(Q^2), \quad (7)$$

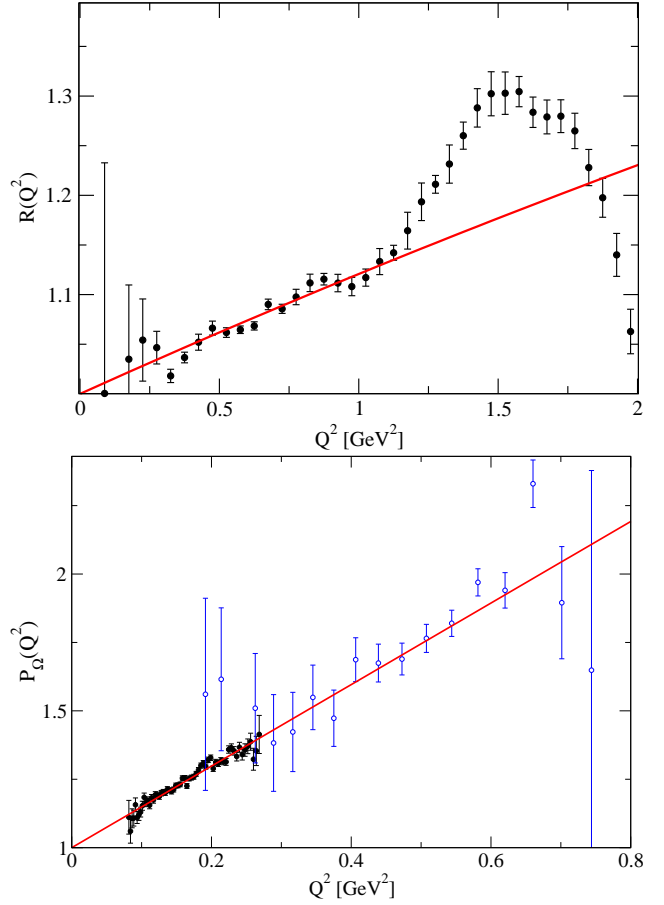


Fig. 1 Upper panel: the function $R(Q^2) = F_V(Q^2)/\Omega(Q^2)$, where data from τ decays from Ref. [9] were used for the pion vector form factor. The red line denotes a linear fit to the data in the kinematic regime from threshold to $s = 1 \text{ GeV}^2$. Lower panel: the function $P_\Omega(Q^2)$ for radiative decays of the η —solid symbols from Ref. [7]—and the η' —open symbols from Ref. [6]. The red line denotes a linear fit to the η data.

where, using $P_\Omega(0) = 1$ and $\Omega(0) = 1$, $\mathcal{A}_{\pi\pi\gamma}^\eta(0) = A_{\pi\pi\gamma}^\eta$.

In Figure 1 we show the Q^2 dependence of $R(Q^2)$ (upper panel) and $P_\Omega(Q^2)$ (lower panel), the latter for η (solid symbols) as well as η' (open symbols) decays. As one can see, $R(Q^2)$ is perfectly linear for $Q^2 < 1 \text{ GeV}^2$. For larger values of the $\pi\pi$ invariant mass squared one finds clear deviations from linearity—in this case caused by the ρ' [10], the first radial excitation of the ρ -meson. The lower panel demonstrates that $P_\Omega(Q^2)$ is linear within the experimental uncertainties in the full range kinematically accessible—although the data for η' clearly call for improvement. The straight line in the figure is a fit to the η data, which demonstrates that the slope of the η' spectrum is consistent with that of the η —this observation will be exploited below.

Whereas $F_V(Q^2)$ does not have a left-hand cut, the decay amplitudes for the radiative decays of η and η' have one—the leading singularity in both cases is driven by the same $\pi\pi\eta$ intermediate state followed by $\pi\eta \rightarrow \pi\gamma$. However, it

is strongly suppressed [3]: on the one hand for kinematical reasons, since the particle pairs in the t -channel have to be (at least) in a relative p -wave, on the other hand for dynamical reasons, since the p -wave $\pi\eta$ interaction starts only at next-to-leading order in the chiral expansion [11, 12]. It is therefore justified to neglect it—an assumption supported by the strict linearity of $P_\Omega(Q^2)$ demonstrated above. Then, analogous to $F_V(Q^2)$, also the ratios of the η and η' amplitudes with respect to the Omnès function should be linear up to about 1 GeV^2 . At least up to $Q^2 = m_{\eta'}^2$, with $m_{\eta'}$ the η' mass, this can be checked experimentally once better data are available for the η' radiative decays—those data should be expected from BES-III [13] and CLAS [14] in the near future. For energies above 1 GeV , some influence from the higher ρ resonances should be expected. In the next section a dispersion integral is derived that allows us, using mainly the input described in this section, to calculate the slope of the $\eta \rightarrow \gamma\gamma^*$ form factor.

Thus, for Q^2 values up to 1 GeV^2 the $\eta \rightarrow \pi\pi\gamma$ transition amplitude is completely fixed by the parameter α and the pion vector form factor. We here use for α the value given in Ref. [7],

$$\alpha = (1.32 \pm 0.13) \text{ GeV}^{-2}. \quad (8)$$

The uncertainty contains the statistical as well as the systematic uncertainty from the data as well as the theoretical uncertainty quoted in Ref. [3]. Below we will need the transition amplitude also for larger values of s . As a consistency check we confirmed that we reproduce the above value for α from our own fit to the data of Ref. [7] using the full vector form factor, $F_V(Q^2)_{e^+e^-}$ of Ref. [10] as input. It includes the effect of isospin violation from γ - ρ mixing (cf. Ref. [15]) as well as ρ - ω and ρ - ϕ mixing and the effect of the first two excited states, ρ' and ρ'' . Clearly, the impact of the higher resonances as well as the mixing with isoscalar vector states may depend on the reaction channel, since there is no reason to expect their effects to be equal in η radiative decays to those found in the e^+e^- reaction. Therefore in our analysis we also used an alternative form-factor parameterization to control the theoretical uncertainty: namely one that is extracted from τ decays, $F_V(Q^2)_\tau$, and therefore does not contain any mixing with ω , ϕ or γ . The spread in the results from using those two form factors is included in the systematic uncertainty reported below.

3 $\eta \rightarrow \gamma\gamma^*$: dispersion relation

The discontinuity of the isovector part of the $\eta \rightarrow \gamma\gamma^*$ decay amplitude is driven by the on-shell two-pion intermediate states, see Figure 2. Especially, one finds

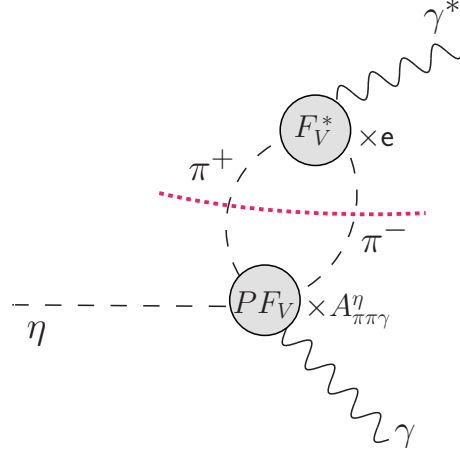


Fig. 2 The isovector part of the $\eta \rightarrow \gamma\gamma^*$ decay amplitude driven by the on-shell two-pion intermediate states. The two-pion cut is indicated by the (red) dotted line. The vertex $F_V P A_{\pi\pi\gamma}^\eta$ indicates the $\eta \rightarrow \pi^+\pi^-\gamma$ transition form factor, while the other vertex corresponds to the two-pion vector form factor F_V^* times the electric charge e , see Eq. (9) for more details.

$$\begin{aligned} \text{Disc } \mathcal{A}^{\rho\mu} &= i(2\pi)^4 \int d\Phi_2 \mathcal{M}^\mu(\eta(p_\eta) \rightarrow \pi^+(p_1)\pi^-(p_2)\gamma(p_\gamma)) \\ &\quad \times \mathcal{M}^{\rho*}(\pi^+(p_1)\pi^-(p_2) \rightarrow \gamma^*(p_\gamma)) \\ &= i(2\pi)^4 \int d\Phi_2 P(Q^2) F_V(Q^2) A_{\pi\pi\gamma}^\eta \varepsilon^{\mu\nu\alpha\beta} (p_\gamma)_\nu (p_1)_\alpha (p_2)_\beta \\ &\quad \times e F_V(Q^2)^* (p_1 - p_2)^\rho \\ &= i(2\pi)^4 e A_{\pi\pi\gamma}^\eta P(Q^2) |F_V(Q^2)|^2 \varepsilon^{\mu\nu\alpha\beta} (p_\gamma)_\nu \\ &\quad \times \int d\Phi_2 (p_1 - p_2)^\rho (p_1)_\alpha (p_2)_\beta, \end{aligned} \quad (9)$$

where e is the unit of electric charge. Defining $k \equiv (p_1 - p_2)/2$ and $Q \equiv p_1 + p_2$ we get

$$\begin{aligned} \text{Disc } \mathcal{A}^{\rho\mu} &= 2i(2\pi)^4 e A_{\pi\pi\gamma}^\eta P(Q^2) |F_V(Q^2)|^2 \varepsilon^{\mu\nu\alpha\beta} (p_\gamma)_\nu \\ &\quad \times \int d\Phi_2 k^\rho k_\alpha Q_\beta. \end{aligned} \quad (10)$$

In the η rest frame ($s_\eta \equiv m_\eta^2$ with m_η the η mass) we have $\mathbf{Q} = -\mathbf{p}_\gamma$ and therefore

$$\varepsilon^{\mu\nu\alpha\beta} (p_\gamma)_\nu Q_\beta = \sqrt{s_\eta} \varepsilon^{mab} Q^b$$

where $\varepsilon_{0123} = -\varepsilon^{0123} = +1$ and m, a, b denote the spatial components for the Lorentz indices μ, α, β , respectively. We thus get, using

$$\begin{aligned} (2\pi)^4 d\Phi_2 k^r k^a &= d\Omega \frac{1}{32\pi^2} \sigma_\pi(Q^2) k^r k^a \\ &= \frac{1}{32\pi^2} \left(\frac{4\pi}{3} \right) \sigma_\pi(Q^2) \mathbf{k}^r \delta^{ra} \end{aligned}$$

$$\text{and } \mathbf{k}^2 = (Q^2 - 4m_\pi^2)/4 = Q^2 \sigma_\pi^2(Q^2)/4,$$

$$\begin{aligned} \text{Disc } \mathcal{A}^{rm} &= 2i\pi e A_{\pi\pi\gamma}^\eta \sqrt{s_\eta} \varepsilon^{mrb} p_\gamma^b \\ &\quad \times \frac{Q^2}{96\pi^2} \sigma_\pi(Q^2)^3 P(Q^2) |F_V(Q^2)|^2. \end{aligned} \quad (11)$$

Due to $\text{Disc } \mathcal{A}^{rm} = 2i \text{Im } \mathcal{A}^{rm}$, we may then write a once-subtracted dispersion integral

$$\mathcal{A}^{rm}(Q^2) = \mathcal{A}^{rm}(0) + eA_{\pi\pi\gamma}^\eta \sqrt{s_\eta} \varepsilon^{mrb} p_\gamma^b \times \frac{Q^2}{96\pi^2} \int_{4m_\pi^2}^\infty ds' \sigma_\pi(s')^3 P(s') \frac{|F_V(s')|^2}{s' - Q^2 - i\varepsilon}. \quad (12)$$

Using $\mathcal{A}^{rm}(0) \equiv \mathcal{A}^{rm}(\eta \rightarrow \gamma\gamma) = A_{\gamma\gamma}^\eta \sqrt{s_\eta} \varepsilon^{mrb} p_\gamma^b$, where

$$A_{\gamma\gamma}^\eta \equiv \sqrt{\Gamma_{\gamma\gamma}^\eta 64\pi/m^3}, \quad (13)$$

the isovector part of the $\eta \rightarrow \gamma\gamma^*$ transition form factor is defined via

$$\mathcal{A}^{rm}(Q^2) = A_{\gamma\gamma}^\eta \sqrt{s_\eta} \varepsilon^{mrb} p_\gamma^b F_{\eta\gamma^*\gamma}^{(I=1)}(Q^2, 0) \quad (14)$$

as

$$F_{\eta\gamma^*\gamma}^{(I=1)}(Q^2, 0) = 1 + \kappa_\eta \left(\frac{Q^2}{96\pi^2 f_\pi^2} \right) \times \int_{4m_\pi^2}^\infty ds' \sigma_\pi(s')^3 P(s') \frac{|F_V(s')|^2}{s' - Q^2 - i\varepsilon}. \quad (15)$$

The pre-factor is specified as $\kappa_\eta \equiv eA_{\pi\pi\gamma}^\eta f_\pi^2 / A_{\gamma\gamma}^\eta$, with $f_\pi = 92.2 \text{ MeV}$ the pion decay constant [4], introduced here for later convenience. Note, in the SU(3) chiral limit one has $\kappa_\eta = 1$. Based on Eq. (13) and Eq. (1) κ_η can be fixed directly from data. The slope parameter $b_\eta^{(I=1)}$ is defined via

$$F_{\eta\gamma^*\gamma}^{(I=1)}(Q^2, 0) = 1 + b_\eta^{(I=1)} Q^2 + \mathcal{O}(Q^4).$$

Thus, from Eq. (15) we get the following integral representation for the isovector component of the slope parameter

$$b_\eta^{(I=1)} = \frac{\kappa_\eta}{6(4\pi f_\pi)^2} \int_{4m_\pi^2}^\infty \frac{ds'}{s'} \sigma_\pi(s')^3 P(s') |F_V(s')|^2. \quad (16)$$

The isovector part of the form factor is model-independent, since it can be expressed fully in terms of experimental observables. Those are the branching ratios (or partial decay widths) of $\eta \rightarrow \pi^+ \pi^- \gamma$ and $\eta \rightarrow \gamma\gamma$, to fix the prefactor κ_η , the slope parameter α from the spectral shape of $\eta/\eta' \rightarrow \pi^+ \pi^- \gamma$ (cf. Ref. [3] and Eq. (8)) and the pion vector form factor. As will be demonstrated below, the uncertainty from our ignorance about the high- Q^2 behavior of both $P(Q^2)$ as well as $F_V(Q^2)$ can be estimated reliably.

4 Model for the isoscalar contribution of the slope parameter

The two-pion contribution is almost purely isovector (up to a small contribution from the ω contributing via ρ - ω mixing). However, the full slope parameter contains also an isoscalar contribution. To quantify this part, a simple model is constructed in the following. It is based on a vector meson dominance (VMD) estimate of this contribution (see Appendix A), as given in Ref. [16].

In particular in Table 4 of Ref. [16] the expression of the total slope of the η transition form factor—calculated in VMD including SU(3) breaking—can be found: the slope includes *both* isovector and isoscalar contributions and is given in terms of the masses m_ρ , m_ω and m_ϕ of the three lowest vector meson resonances (the isovector ρ and the isoscalar ω and ϕ) by

$$b_\eta^{(\text{VMD})} = \frac{m_\rho^{-2}}{1 + \frac{1}{9} - \frac{\sqrt{2}}{3} \beta_\eta} + \frac{\frac{1}{9} m_\omega^{-2} - \frac{\sqrt{2}}{3} \beta_\eta m_\phi^{-2}}{1 + \frac{1}{9} - \frac{\sqrt{2}}{3} \beta_\eta} \approx 1.8 \text{ GeV}^{-2} \quad (17)$$

in terms of a one-angle η - η' mixing scheme

$$\beta_\eta = \frac{2}{3} \left[\frac{\sqrt{2} \cos \theta_P + \sin \theta_P}{\cos \theta_P - \sqrt{2} \sin \theta_P} \right] = \frac{\sqrt{2}}{3} \approx 0.47. \quad (18)$$

Here we applied the standard value in chiral perturbation theory (ChPT),

$$\theta_P = \arcsin(-1/3) \approx -19.5^\circ,$$

see, e.g., Ref. [17], for the mixing angle θ_P of the pseudoscalar nonet. This value is consistent with both a one-loop analysis for the mass matrix and the two-photon decays of η and η' [18].

Since the isovector contribution has been determined in Sect. 3 in a model-independent way, we here replace the VMD isovector (*i.e.* ρ meson) contribution to the slope parameter—the first term on the r.h.s. of Eq. (17)—by the model-independent integral representation (16) based on the vector form factor (15), while we preserve the isoscalar term of Ref. [16]—the second term on the r.h.s. of Eq. (17). The resulting expression for the total slope of the η transition form factor is then given by

$$b_\eta = b_\eta^{(I=1)} + \frac{\frac{1}{9} m_\omega^{-2} - \frac{\sqrt{2}}{3} \beta_\eta m_\phi^{-2}}{1 + \frac{1}{9} - \frac{\sqrt{2}}{3} \beta_\eta} \approx b_\eta^{(I=1)} - 0.036 \text{ GeV}^{-2}. \quad (19)$$

The isoscalar component in Eq. (19) turns out to be smaller than the uncertainty of our full calculation, when the standard value for the mixing angle, $\theta_P = -\sin(1/3) \approx -19.5^\circ$, is used. In case of the η' , however, the mixing angle -19.5° leads to a positive and comparably large isoscalar shift of 0.39 GeV^{-2} , since $-\beta_{\eta'} \sqrt{2}/3 = -2/9$ in Eq. (17) has to be replaced by $+\beta_{\eta'} \sqrt{2}/3 = +4/9$ with $\beta_{\eta'} = 4/(9\beta_\eta) = 2\sqrt{2}/3$.

In a recent analysis of a large set of data, Refs. [19, 20] report a mixing angle of about -10.5° (see also Refs. [21, 22]). However, within that approach other parameters change as well and, based on this model, one gets, respectively, $b_\eta^{(I=0)} = -0.023 \text{ GeV}^{-2}$ and $b_{\eta'}^{(I=0)} = 0.30 \text{ GeV}^{-2}$ —rather

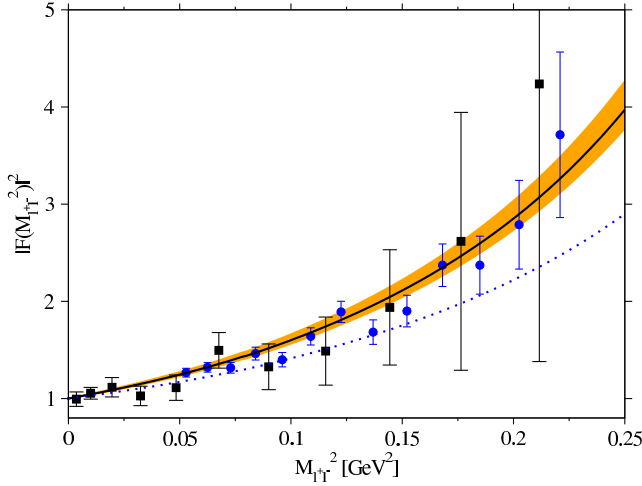


Fig. 3 The squared modulus of the $\eta \rightarrow \gamma\gamma^*$ transition form factor as function of the invariant mass square, $M_{l^+l^-}^2$, of the (electron or muon) dilepton pair from the subsequent decay $\gamma^* \rightarrow l^+l^-$. The results of Eq. (15) inserted into Eq. (20) are compared with the two most recent measurements from Refs. [23, 24], which are displayed as solid dots and squares, respectively. The (orange) band shows the spread of our results emerging from the uncertainty in α (deduced from a fit to $\eta \rightarrow \pi\pi\gamma$ of Ref. [7]—cf. Eq. (8)), from the variation of the end point s_{\max} of the integral (from $m_{\eta'}^2$ to 2 GeV^2), the applied form factors and the uncertainties of branching ratios entering the prefactor. Solid line: our central result (with $\alpha = 1.32\text{ GeV}^{-2}$, and $s_{\max} = 1\text{ GeV}^2$). Dotted line: dispersion integral with $\alpha = 0$ and $s_{\max} = 1\text{ GeV}^2$.

close to the values given above. The spread between the two different results for the isoscalar contributions will be included in the uncertainties. If, on the other hand, we had used an angle of -10.5° directly in Eq. (19), the isoscalar correction to b_η would have been as large as -0.15 GeV^{-2} while that to $b_{\eta'}$ would have been 0.34 GeV^{-2} .

Applying the model-dependent isoscalar contribution of Eq. (19), the total transition form factor of the η reads

$$F_{\eta\gamma^*\gamma}^{\text{total}}(Q^2) = F_{\eta\gamma^*\gamma}^{(I=1)}(Q^2) + \frac{1}{8} \left(\frac{Q^2}{m_\omega^2 - Q^2 - im_\omega\Gamma_\omega} - \frac{2Q^2}{m_\phi^2 - Q^2 - im_\phi\Gamma_\phi} \right), \quad (20)$$

where the model-independent expression of the isovector contribution of the η transition form factor (15) is selected as the first term. Γ_ω and Γ_ϕ are the total widths of the ω and ϕ meson, respectively, as given in Ref. [4]. Note that neither the model-independent isovector part (15) nor the additional isoscalar contributions (20) to the η transition form factor vanish in the limit $Q^2 \rightarrow \infty$. This fact is closely tied to the choice of the *once-subtracted* form of the dispersion integral in Sect. 3 that has the inherent property that the subtraction constant must be determined by empirical input. In fact, we rather prefer to determine the transition form factor from the correct low-energy empirical input than to rely on a loose extrapolation to perturbative QCD which favours the vanishing of the transition form factor at $Q^2 \rightarrow \infty$ [25, 26, 27].

5 Results

The uncertainties for the evaluation of the isovector part of the transition form factor emerge from those of the experimental branching fractions (collected in the prefactor κ_η) and from the value of α (cf. Eq. (8)).

Formally the integral of Eq. (15) runs up to infinity. On the other hand we can control its input, especially $P(Q^2)$, only in the regime up to $Q^2 = 1\text{ GeV}^2$. In order to demonstrate that the relevant contributions indeed come from the regime below 1 GeV^2 , we follow Refs. [28, 29] and investigate the *un-subtracted* dispersion integral, analog to Eq. (12), which provides a sum rule for $A_{\gamma\gamma}^\eta$. Namely the isovector part of the $\eta \rightarrow \gamma\gamma$ amplitude should satisfy

$$A_{\gamma\gamma}^{\eta(I=1)} = e A_{\pi\pi\gamma}^\eta \frac{1}{96\pi^2} \int_{4m_\pi^2}^{\infty} ds' \sigma_\pi(s')^3 P(s') |F_V(s')|^2. \quad (21)$$

If according to methods of Ref. [16] the *model-dependent* isoscalar contribution is included, the sum rule—with $A_{\gamma\gamma}^{\eta(I=1)}$ as above—becomes instead

$$A_{\gamma\gamma}^\eta = A_{\gamma\gamma}^{\eta(I=1)} - \frac{1}{8} A_{\gamma\gamma}^\eta. \quad (22)$$

Here the last term is derived in analogy to the corresponding expression in Eq. (19) from

$$\frac{\frac{1}{9} - \frac{\sqrt{2}}{3}\beta_\eta}{1 + \frac{1}{9} - \frac{\sqrt{2}}{3}\beta_\eta} \xrightarrow{\beta_\eta = \sqrt{2}/3} -\frac{1}{8} \quad (23)$$

if the standard mixing angle $\theta = \arcsin(-1/3)$ is inserted in β_η .

If $P(s)$ were linear up to infinite energies, the integral in (21) would be formally log-divergent, since $F_V(s) \sim 1/s$ for large values of s . However, the goal here is to confirm that all relevant physics is located below 1 GeV^2 . And indeed, if the pertinent integral in Eq. (21) is truncated at 1 GeV^2 , the right-hand side of the sum rule (22) overestimates the left-hand one by only $(6 \pm 4)\%$. If it is truncated already at $s = m_{\eta'}^2$, the mismatch between the right-hand and left-hand side is only $(1.5 \pm 3.5)\%$. This provides strong evidence that the *once-subtracted* integral of Eq. (16) and thus also of Eq. (15) should provide reliable results, when being cut at or slightly below 1 GeV^2 . For the η decay the isoscalar contribution turns out to be negligible.

To get a conservative estimate for the possible impact of higher values of s in the integral, we also evaluated the integral using $s_{\max} = 2\text{ GeV}^2$ —an increase to $s_{\max} = 3\text{ GeV}^2$ did not alter the displayed results. For that purpose we continue $P(s)$ linearly in combination with the two form factors $F_V(Q^2)_{e^+e^-}$, and $F_V(Q^2)_\tau$ introduced at the end of Sect. 2. This procedure lead to some increase in the form factor, the largest results were obtained with the maximum input value for α from Eq. (8) in combination with the τ form factor, $F_V(Q^2)_\tau$.

Table 1 Comparison of our result for the slope parameter b_η as given in Eq. (25) with experimental as well as previous theoretical investigations. The results for the theoretical works (except [30]) are taken from Table II of Ref. [31]. The experimental result $b_\eta = (1.6 \pm 2.0) \text{ GeV}^{-2}$ of Ref. [32] (for the process $\eta \rightarrow e^+ e^- \gamma$) is not included because of its large uncertainty.

Type	Process	Ref.	$b_\eta [\text{GeV}^{-2}]$	
Exp.	$\eta \rightarrow \mu^+ \mu^- \gamma$	[33]	1.90 ± 0.40	
Exp.	$e^+ e^- \rightarrow e^+ e^- \gamma \gamma^* \rightarrow e^+ e^- \eta$	[34]	2.04 ± 0.47	
Exp.	$e^+ e^- \rightarrow e^+ e^- \gamma \gamma^* \rightarrow e^+ e^- \eta$	[35]	1.42 ± 0.20	
Exp.	$\eta \rightarrow \mu^+ \mu^- \gamma$	[36]	1.95 ± 0.17	
Exp.	$\eta \rightarrow \mu^+ \mu^- \gamma$	[23]	1.95 ± 0.07	
Exp.	$\eta \rightarrow e^+ e^- \gamma$	[24]	1.92 ± 0.37	
Theory	VMD	[37,38,39]	1.78	
Theory	Quark loop	[37,38,39]	1.69	
Theory	Brodsky-Lepage	[25]	1.21	
Theory	1-loop ChPT	[31]	1.69	
Theory	Padé approx. fit to [35,40,41] data	[30]	$1.99 \pm 0.16 \pm 0.11$	
Theory	Dispersion integral	This work	$2.05^{+0.22}_{-0.10}$	

The resulting spread for the $\eta \rightarrow \gamma \gamma^*$ transition form factor that emerges from the calculation, including the uncertainties mentioned above and with the upper limit of integration varied from $s_{\text{max}} = m_{\eta'}^2$ to 2 GeV^2 , is shown as the (orange) band in Figure 3.

The formalism allows one to disentangle effects from the $\pi\pi$ -interactions, which are universal, from those of the decay vertex, which are reaction specific. Thus it is interesting to investigate how much of the form factor emerges from the two-pion interactions and how much from the production vertex. We therefore show as the (blue) dotted line in Figure 3 the result for $\alpha = 0$. Thus about 20% of the slope of the η transition form factor results from the decay vertex while 80% come from the $\pi\pi$ interactions.

The isovector contribution of the slope of the transition amplitude is determined to be

$$b_\eta^{(I=1)} = (2.09^{+0.21}_{-0.11}) \text{ GeV}^{-2}. \quad (24)$$

The uncertainties include those of the branchings, the parameter α , the form factor as well as the range of integration. If the isoscalar contribution is added to $b_\eta^{(I=1)}$, we get

for the full slope of the transition form factor

$$b_\eta = (2.05^{+0.22}_{-0.10}) \text{ GeV}^{-2} \quad (25)$$

for the standard value for the η - η' mixing angle $\theta_P = -19.5^\circ$. The uncertainties are analogous to those shown in Eq. (24). The result (25) is compatible with all recent experimental results, but bigger than most of the previous theoretical studies, except the recent one of Ref. [30] using Padé approximants to analyze the data of Refs. [35,40,41], see Table 1.

At present the data available for $\eta' \rightarrow \pi\pi\gamma$ are not good enough to constrain the slope parameter α of Eq. (2) sufficiently to repeat the analysis from above also for the η' . However, as suggested by the existing data—*cf.* lower panel of Figure 1—as well as by the fact that $\eta \rightarrow \pi\pi\gamma$ and $\eta' \rightarrow \pi\pi\gamma$ have the same leading left-hand cut, we may now assume that the value of α given in Eq. (8) also applies to radiative η' decays. Then, the only thing that changes compared to the analysis above is the pre-factor κ_η in Eq. (16) which is replaced by $\kappa_{\eta'} \equiv e A_{\pi\pi\gamma}^{\eta'} f_\pi^2 / A_{\gamma\gamma}^{\eta'}$ where the ratio of amplitude factors $A_{\pi\pi\gamma}^{\eta'}$ and $A_{\gamma\gamma}^{\eta'}$ follows from ratio of the square roots of the corresponding branching ratios. In this

Table 2 Comparison of our result for the slope parameter $b_{\eta'}$ as given in Eq. (27) with experimental as well as previous theoretical investigations, under the additional assumption that the parameter α , cf. Eq. (2), is the same for both η and η' decays. The results for the various experimental and theoretical works (except [30]) are taken from Ref. [31].

Type	Process	Ref.	$b_{\eta'} [\text{GeV}^{-2}]$	
Exp.	$\eta' \rightarrow \mu^+ \mu^- \gamma$	[42,33]	1.69 ± 0.79	
Exp.	$e^+ e^- \rightarrow e^+ e^- \gamma \gamma^* \rightarrow e^+ e^- \eta'$	[34]	1.38 ± 0.23	
Exp.	$e^+ e^- \rightarrow e^+ e^- \gamma \gamma^* \rightarrow e^+ e^- \eta'$	[35]	1.60 ± 0.16	
Theory	VMD	[37,38,39]	1.45	
Theory	Quark loop	[37,38,39]	1.42	
Theory	Brodsky-Lepage	[25]	2.30	
Theory	1-loop ChPT	[31]	1.60	
Theory	Padé approx. fit to [35,40,41] data	[30]	$1.49 \pm 0.17 \pm 0.09$	
Theory	Dispersion integral	This work	$1.58^{+0.18}_{-0.13}$	

way we get

$$b_{\eta'}^{(I=1)} = (1.19^{+0.10}_{-0.04}) \text{GeV}^{-2}, \quad (26)$$

where the theoretical uncertainty is estimated in the same way as in the η case. If again the isoscalar contribution is added, the full slope of the transition form factor is given by

$$b_{\eta'} = (1.58^{+0.18}_{-0.13}) \text{GeV}^{-2} \quad (27)$$

where again we used the standard value for the η - η' mixing angle $\theta_P = -19.5^\circ$. The increase in the uncertainty takes care of the change of the isoscalar contribution when the mixing scheme of Refs. [19,20] is applied. The result (27) is compatible with all experimental results, especially with the Padé-approximants fit [30] to the [35,40,41] data and with the predictions of 1-loop ChPT as well as VMD, see Table 2.

As a test of internal consistency, we evaluated the analogous sum rule to Eq. (22) also for the η' . In fact, if the integral occurring in the η' analog of Eq. (21), namely in the isovector part of the sum rule, is again truncated at 1 GeV^2 , the right-hand side of the total $A_{\gamma\gamma}^{\eta'}$ sum rule,

$$A_{\gamma\gamma}^{\eta'} = A_{\gamma\gamma}^{\eta'(I=1)} + \frac{5}{14} A_{\gamma\gamma}^{\eta'}, \quad (28)$$

which also contains a model-dependent isoscalar term, overestimates the left-hand one by only $(3 \pm 1)\%$. If the integral is already truncated at $s = m_{\eta'}^2$, the mismatch becomes only $(1 \pm 1)\%$.

6 Summary and discussion

In summary, we have derived a model-independent integral representation for the isovector contribution to the $\eta \rightarrow \gamma\gamma^*$ transition form factor at low energies and especially the corresponding slope parameter b_η . The necessary input was taken directly from experimental data, namely from the pion vector form factor, the tabulated branching ratios for the $\eta \rightarrow \gamma\gamma$ and $\eta \rightarrow \pi^+ \pi^- \gamma$ decays, and from the measured spectral shape of the latter process, parametrized by just one coefficient, the slope parameter α as described in Ref. [3] and Eq. (2).

This was possible with the help of the machinery of dispersion theory, by utilizing the fact that the pion vector form factor and the $\eta \rightarrow \pi^+ \pi^- \gamma$ (and $\eta' \rightarrow \pi^+ \pi^- \gamma$) decay amplitudes have the same right-hand cut—at least in the region below 1 GeV^2 for the invariant pion mass square, the region dominating the *once*-subtracted dispersion relation. As a consistency check we demonstrated that a related *un*-subtracted dispersion integral is saturated at 1 GeV^2 .

The isoscalar contribution of the slope parameter b_η , modelled by a simple vector-meson-dominance approximation, turned out to be smaller than the uncertainty of the calculation for the isovector part in the η case. In the η' scenario, the isoscalar part was larger, but still of subleading nature. In addition, the isoscalar contributions when added to the isovector ones helped in saturating the *un*-subtracted

$\eta \rightarrow \gamma\gamma$ and $\eta' \rightarrow \gamma\gamma$ sum rules below 1 GeV^2 to an uncertainty better than 10% and 4%, respectively.

Our final results for the slopes of the η transition form factor are $b_\eta^{(I=1)} = (2.09_{-0.11}^{+0.21}) \text{ GeV}^{-2}$ for the isovector contribution and $b_\eta = (2.05_{-0.10}^{+0.22}) \text{ GeV}^{-2}$ in total. In fact, the slope at the origin of the transition form factor following the lower edge of the (orange) band in Figure 3 corresponds to our prediction for the lower bound on the slope parameter, *i.e.* $b_\eta \geq 1.95 \text{ GeV}^{-2}$. This value is compatible with all recent experimental results, but bigger than most previous theoretical studies known to us.

The available data for the $\eta' \rightarrow \pi\pi\gamma$ spectral shape are not good enough to allow for a compatible fit of the corresponding α parameter. However, the slope parameter α solely determined from the high-precision $\eta \rightarrow \pi\pi\gamma$ data of Ref. [7] also provided a good fit to the available $\eta' \rightarrow \pi\pi\gamma$ spectral data—without any readjustment. Therefore, we conjectured that the value of α determined in $\eta \rightarrow \pi\pi\gamma$ also applies to $\eta' \rightarrow \pi\pi\gamma$.

Under this assumption and the inclusion of the model-dependent but subleading isoscalar contributions, which were derived in the same way as for the η , the following results apply for the slope parameter $b_{\eta'}$: the isovector contribution reads $b_{\eta'}^{(I=1)} = (1.19_{-0.04}^{+0.10}) \text{ GeV}^{-2}$ while the total result is $b_{\eta'} = (1.58_{-0.13}^{+0.18}) \text{ GeV}^{-2}$, where the freedom in the choice of mixing scheme led to the increase in the uncertainty. Otherwise the uncertainties are calculated as in the η case. Our result for $b_{\eta'}$ is bigger than the VMD predictions, but compatible with all known experimental data, which, however, are rather old, and—this time—also with chiral perturbation theory truncated at 1-loop order.

In case of the η slope parameter there seems to be some tension between the values determined from experimental data and the ones calculated by the dispersion integral. However, in this context it should be stressed that the empirical slopes have been extracted from experimental data usually with the help of monopole fits. Those have typically a larger curvature than our main result—*cf.* (orange) band in Figure 3. Thus, when the slope at $Q^2 = 0$ is extracted from a monopole fit of the data, say well above the $\mu^+\mu^-$ threshold, the results are characteristically smaller than those derived from the functional form of our final result.

The formalism presented here allows us to disentangle the effects on the form factor slope emerging from the $\pi\pi$ -interaction, which are universal, from those of the production vertex, which are reaction specific. Our results show that the production vertex itself, whose effect is encoded in the parameter α , contributes to about 20% of the slope of the transition form factor, while the bulk is provided by the $\pi\pi$ intermediate state, which might be viewed as coming from the pole of ρ -meson. Therefore, parametrizing the transition form factor as a single monopole term, which suggests that

the mass scale relevant for $\eta \rightarrow \gamma\gamma^*$ is entirely controlled by a single, reaction dependent scale, is misleading, since the actual shape of the form factor emerges from the interplay of two scales.

Acknowledgements We would like to thank Martin Hoferichter, Bastian Kubis and Franz Niecknig for helpful discussions and advice. We are grateful to Camilla Di Donato for providing the KLOE data and to Marc Unverzagt for help in connection with Figure 3. This work is supported in part by the DFG and the NSFC through funds provided to the Sino-German CRC 110 “Symmetries and the Emergence of Structure in QCD”, and by the European Community-Research Infrastructure Integrating Activity “Study of Strongly Interacting Matter” (acronym HadronPhysics3).

Appendix A: Comparison with the vector meson dominance approximation

It is instructive to compare Eq. (16) with what can be derived from a simple realization of vector meson dominance (VMD). For this purpose, we may write

$$P(s)^{\text{VMD}} = 1 \quad (i.e.: \alpha = 0), \quad (\text{A.1})$$

$$F_V(s)^{\text{VMD}} = \frac{m_\rho^2}{m_\rho^2 - s - im_\rho \Gamma_\rho(s)}, \quad (\text{A.2})$$

$$\kappa_\eta^{\text{VMD}} = 1 \quad (i.e.: A_{\gamma\gamma}^\eta = e A_{\pi\pi\gamma}^\eta f_\pi^2). \quad (\text{A.3})$$

To proceed we use $\pi\delta(x - x_0) = \lim_{\varepsilon \rightarrow 0} \frac{\varepsilon}{(x - x_0)^2 + \varepsilon^2}$ to approximate the form factor square with the help of the substitution $\varepsilon \equiv m_\rho \Gamma_\rho(s')$ as follows:

$$\begin{aligned} |F_V(s')^{\text{VMD}}|^2 &= \frac{m_\rho^4}{(m_\rho^2 - s')^2 + m_\rho^2 \Gamma_\rho(s')^2} \\ &= \frac{m_\rho^3}{\Gamma_\rho(s')} \frac{\varepsilon}{(m_\rho^2 - s')^2 + \varepsilon^2} \approx \frac{m_\rho^3}{\Gamma_\rho(s')} \pi\delta(s' - m_\rho^2). \end{aligned} \quad (\text{A.4})$$

Inserting (A.1), (A.3) and (A.4) into Eq. (16) yields

$$\begin{aligned} b_{\eta}^{(I=1)} \text{VMD} &\approx \frac{1}{96\pi^2 f_\pi^2} \int_{4m_\pi^2}^\infty \frac{ds'}{s'} \sigma_\pi(s')^3 \frac{m_\rho^3}{\Gamma_\rho(s')} \pi\delta(s' - m_\rho^2) \\ &= \frac{1}{96\pi f_\pi^2} \frac{m_\rho}{\Gamma_\rho(m_\rho^2)} \left(\sigma_\pi(m_\rho^2)\right)^3. \end{aligned} \quad (\text{A.5})$$

We may now employ the explicit form of the width of ρ ,

$$\Gamma_\rho(m_\rho^2) = \frac{1}{48\pi} g_{\rho\pi\pi}^2 m_\rho \left(\sigma_\pi(m_\rho^2)\right)^3, \quad (\text{A.6})$$

namely the (spin-averaged) standard two-body decay formula [4] with $\mathcal{M}(\rho^0 \rightarrow \pi^+(p_1)\pi^-(p_2)) = g_{\rho\pi\pi} |\mathbf{p}_1 - \mathbf{p}_2|$ as amplitude and $g_{\rho\pi\pi}$ as coupling constant. In this way we get

$$b_{\eta}^{(I=1)} \text{VMD} \approx \frac{1}{2f_\pi^2 g_{\rho\pi\pi}^2} \approx \frac{1}{m_\rho^2}, \quad (\text{A.7})$$

where in the last step the KSFR relation $g_{\rho\pi\pi}^2 \approx m_\rho^2/(2f_\pi^2)$ was applied [43, 44].

Thus our formalism naturally matches onto the VMD approximation—see, *e.g.*, Refs. [16, 45] for reviews and [19, 20, 21, 22, 46, 47] for recent updates—once the corresponding expressions for the various ingredients are imposed. If we had kept the empirical value $\kappa_\eta = 0.566 \pm 0.006$ and inserted the linear polynomial $P(s') = 1 + \alpha s'$ instead of Eq. (A.1) into the integral of Eq. (A.5), we would have got the modified approximation

$$b_{\eta \text{ mod. VMD}}^{(I=1)} \approx \frac{\kappa_\eta}{m_\rho^2} (1 + \alpha m_\rho^2). \quad (\text{A.8})$$

for the isovector part of the slope. In this case the VMD result would be enlarged by a factor $1 + \alpha m_\rho^2 \approx 1.91 \pm 0.04$, namely by the linear polynomial $P(s')$ evaluated at $s' = m_\rho^2$ with α as in Eq. (8), while the empirical prefactor κ_η would nearly counterbalance this result, such that approximately the original VMD result,

$$b_{\eta \text{ mod. VMD}}^{(I=1)} \approx (1.08 \pm 0.03)/m_\rho^2 \approx (1.80 \pm 0.04) \text{ GeV}^{-2}, \quad (\text{A.9})$$

reemerges. The latter is—as expected—markedly smaller than our prediction (24) from the dispersion integral (16).

References

1. E. Czerwinski et al., arXiv:1207.6556 [hep-ph]
2. H. Czyż et al., arXiv:1306.2045 [hep-ph]
3. F. Stollenwerk, C. Hanhart, A. Kupść, U.-G. Meißner, A. Wirzba, Phys. Lett. B **707**, 184 (2012) [arXiv:1108.2419 [nucl-th]]
4. J. Beringer et al. (Particle Data Group Collaboration), Phys. Rev. D **86**, 010001 (2012) and 2013 partial update for the 2014 edition
5. P. Adlarson et al. (WASA-at-COSY Collaboration), Phys. Lett. B **707**, 243 (2012) [arXiv:1107.5277 [nucl-ex]]
6. A. Abele et al. (Crystal Barrel Collaboration), Phys. Lett. B **402**, 195 (1997)
7. D. Babusci et al. (KLOE/KLOE-2 Collaboration), Phys. Lett. B **718**, 910 (2013) [arXiv:1209.4611 [hep-ex]]
8. R. Garcia-Martin et al., Phys. Rev. D **83**, 074004 (2011) [arXiv:1102.2183 [hep-ph]]
9. M. Fujikawa et al. (Belle Collaboration), Phys. Rev. D **78**, 072006 (2008) [arXiv:0805.3773 [hep-ex]]
10. C. Hanhart, Phys. Lett. B **715**, 170 (2012) [arXiv:1203.6839 [hep-ph]]
11. V. Bernard, N. Kaiser, U.-G. Meißner, Phys. Rev. D **44**, 3698 (1991)
12. B. Kubis, S.P. Schneider, Eur. Phys. J. C **62**, 511 (2009)
13. D.M. Asner et al., Int. J. Mod. Phys. A **24**, S1 (2009) [arXiv:0809.1869 [hep-ex]]
14. P. Adlarson, M. Amaryan, M. Bashkanov, F. Bergmann, M. Berlowski, J. Bijnens, L.C. Balkestaal, D. Coderre et al., arXiv:1204.5509 [nucl-ex]
15. F. Jegerlehner, R. Szafron, Eur. Phys. J. C **71**, 1632 (2011)
16. L.G. Landsberg, Phys. Rep. **128**, 301 (1985)
17. J. Bijnens, A. Bramon, F. Cornet, Phys. Lett. B **237**, 488 (1990)
18. B.R. Holstein, Phys. Scripta T **99**, 55 (2002)
19. M. Benayoun, P. David, L. DelBuono, O. Leitner, H.B. O’Connell, Eur. Phys. J. C **55**, 199 (2008) [arXiv:0711.4482 [hep-ph]]
20. M. Benayoun, P. David, L. DelBuono, O. Leitner, Eur. Phys. J. C **65**, 211 (2010) [arXiv:0907.4047 [hep-ph]]
21. M. Benayoun, L. DelBuono, H.B. O’Connell, Eur. Phys. J. C **17**, 593 (2000) [hep-ph/9905350]
22. M. Benayoun, P. David, L. DelBuono, F. Jegerlehner, Eur. Phys. J. C **72**, 1848 (2012) [arXiv:1106.1315 [hep-ph]]
23. G. Usai (NA60 Collaboration), Nucl. Phys. A **855**, 189 (2011)
24. H. Berghauer, V. Metag, A. Starostin, P. Aguar-Bartolome, L.K. Akasoy, J.R.M. Annand, H.J. Arends, K. Bantawa et al., Phys. Lett. B **701**, 562 (2011)
25. S.J. Brodsky, G.P. Lepage, Phys. Rev. D **24**, 1808 (1981)
26. S.J. Brodsky, F.-G. Cao, G.F. de Teramond, Phys. Rev. D **84**, 033001 (2011) [arXiv:1104.3364 [hep-ph]]
27. J. Bijnens, F. Persson, hep-ph/0106130
28. S.P. Schneider, B. Kubis, F. Niecknig, Phys. Rev. D **86**, 054013 (2012) [arXiv:1206.3098 [hep-ph]]
29. M. Hoferichter, B. Kubis, D. Sakas, Phys. Rev. D **86**, 116009 (2012) [arXiv:1210.6793 [hep-ph]]
30. R. Escribano, P. Masjuan, P. Sanchez-Puertas, arXiv:1307.2061 [hep-ph]
31. L. Ametller, J. Bijnens, A. Bramon, F. Cornet, Phys. Rev. D **45**, 986 (1992)
32. M.N. Achasov, V.M. Aulchenko, K.I. Beloborodov, A.V. Berdyugin, A.G. Bogdanchikov, A.V. Bozhenok, A.D. Bukin, D.A. Bukin et al., Phys. Lett. B **504**, 275, (2001)
33. R.I. Dzhelyadin, S.V. Golovkin, V.A. Kachanov, A.S. Konstantinov, V.F. Konstantinov, V.P. Kubarovsky, A.V. Kulik, L.G. Landsberg et al., Phys. Lett. B **94**, 548 (1980) [Sov. J. Nucl. Phys. **32**, 516 (1980)] [Yad. Fiz. **32**, 998 (1980) 998]
34. H. Aihara et al. (TPC/Two Gamma Collaboration), Phys. Rev. Lett. **64**, 172 (1990)
35. H.J. Behrend et al. (CELLO Collaboration), Z. Phys. C **49**, 401 (1991)
36. R. Arnaldi et al. (NA60 Collaboration), Phys. Lett. B **677**, 260 (2009) [arXiv:0902.2547 [hep-ph]]
37. A. Bramon, E. Masso, Phys. Lett. B **104**, 311 (1981)
38. L. Ametller, L. Bergstrom, A. Bramon, E. Masso, Nucl. Phys. B **228**, 301 (1983)
39. A. Pich, J. Bernabeu, Z. Phys. C **22**, 197 (1984)
40. J. Gronberg et al. (CLEO Collaboration), Phys. Rev. D **57**, 33 (1998) [hep-ex/9707031]
41. P. del Amo Sanchez et al. (BaBar Collaboration), Phys. Rev. D **84**, 052001 (2011) [arXiv:1101.1142 [hep-ex]]
42. R.I. Dzhelyadin, S.V. Golovkin, M.V. Gritsuk, V.A. Kachanov, D.B. Kakauidze, A.S. Konstantinov, V.F. Konstantinov, V.P. Kubarovsky et al., Phys. Lett. B **88**, 379 (1979) [JETP Lett. **30**, 359 (1979)]
43. K. Kawarabayashi, M. Suzuki, Phys. Rev. Lett. **16**, 255 (1966)
44. Riazuddin, Fayyazuddin, Phys. Rev. **147**, 1071 (1966)
45. U.-G. Meißner, Phys. Rep. **161**, 213 (1988)
46. C. Terschläusen, S. Leupold, Phys. Lett. B **691**, 191 (2010) [arXiv:1003.1030 [hep-ph]]
47. C. Terschläusen, S. Leupold, M.F.M. Lutz, arXiv:1204.4125v2 [hep-ph]